PHYSICAL REVIEW D **81,** 123505 (2010)

Inflation and reheating in spontaneously generated gravity

A. Cerioni,[1,2] F. Finelli,[3,2] A. Tronconi,[1,2] and G. Venturi[1,2]

[1]*Dipartimento di Fisica, Università degli Studi di Bologna, via Irnerio, 46-I-40126 Bologna, Italy*

[2]*INFN, Sezione di Bologna, via Irnerio 46, I-40126 Bologna, Italy*

[3]*INAF/IASF Bologna, Istituto di Astrofisica Spaziale e Fisica Cosmica di Bologna, via Gobetti 101, I-40129 Bologna, Italy*

(Received 10 February 2010; published 4 June 2010)

Inflation is studied in the context of induced gravity (IG) $\gamma\sigma^2 R$, where R is the Ricci scalar, σ a scalar field and γ a dimensionless constant, and diverse symmetry-breaking potentials $V(\sigma)$ are considered. In particular we compared the predictions for Landau-Ginzburg and Coleman-Weinberg type potentials and their possible generalizations with the most recent data. We find that large field inflation generally leads to fewer constraints on the parameters and the shape of the potential whereas small field inflation is more problematic and, if viable, implies more constraints, in particular, on the parameter γ. We also examined the reheating phase and obtained an accurate analytical solution for the dynamics of the inflaton and the Hubble parameter by using a multiple scale analysis. The solutions were then used to study the average expansion of the Universe, the average equation of state for the scalar field and both the perturbative and resonant decays of the inflaton field.

DOI: 10.1103/PhysRevD.81.123505 PACS numbers: 98.80.Cq

I. INTRODUCTION

Many years ago a model for a varying gravitational coupling was introduced [1]. The model consisted of a massless scalar field whose inverse was associated with the gravitational coupling. Such a field evolved dynamically in the presence of matter and led to cosmological predictions differing from Einstein gravity (EG) in that one generally obtained a power-law time dependence for the gravitational coupling. Subsequently it was suggested that the gravitational constant is generated as a one-loop effect in some fundamental interaction [2] or through spontaneous symmetry breaking (for reviews see [3,4]). In order to reduce the strong time dependence in a cosmological setting, which remained after the introduction of matter, a simple globally scale invariant model for induced gravity (IG) involving a scalar field σ and a quartic potential $\lambda\sigma^4$ was introduced [5]. The spontaneous breaking of scale invariance in such a context, either through the presence of a condensate [6–8] or quantum effects [9,10], then led to EG plus a cosmological constant and, on treating matter as a perturbation, a time dependence for the scalar field (gravitational constant) and consistent results [5]. A more detailed analysis [11] of such a simple model including both radiation and matter showed that it led to EG plus a cosmological constant as a stable attractor among homogeneous cosmologies and was therefore a viable dark energy model for a range of scalar field initial conditions and a positive γ coupling to the Ricci scalar $\gamma\sigma^2 R$. In that earlier study we considered values for the scalar field which were sufficiently close to the spontaneously broken symmetry equilibrium values for the scalar field and compared our results with present values of the cosmological constant and the solar system data. In a later paper [12] we studied the above approach for values of our parameters sufficiently far from the equilibrium values (back in time) for sufficient inflation and the subsequent reheating to take place and examined the compatibility of the predictions for different symmetry-breaking potentials with the current data.

The aim of this paper is to investigate in detail the dynamics of the scalar field and the generation of scalar and tensor perturbations in the early Universe. The paper is organized as follows: in Sec. II the formalism and the general equations for the homogeneous dynamics are described. In Sec. III we formalize the problem of perturbations in the IG context, and Sec. IV is dedicated to comparing the predictions of diverse symmetry-breaking potentials with the most recent data. In Sec. V we apply a multiple scale analysis (MSA) to the phase of coherent oscillations of the inflaton field at the end of inflation. In Sec. VI we study the perturbative decay of the inflaton field in the IG context, and in Sec. VII the resonant decay of the inflaton is discussed. Finally, in Sec. VIII, our conclusions are summarized.

II. IG INFLATION

We consider the system described by the action

$$S = \int d^4x\sqrt{-g}\left[-\frac{g^{\mu\nu}}{2}\partial_\mu\sigma\partial_\nu\sigma + \frac{\gamma}{2}\sigma^2 R - V(\sigma)\right] \quad (1)$$

where γ is a dimensionless, positive definite parameter giving the nonminimal coupling between the scalar field and gravity. The Einstein-Hillbert term for gravity is replaced by an effective masslike term for the scalar field σ. In turn such a scalar field is also responsible for the existence of space-time curvature and its expectation value dynamically generates an effective Planck mass. If we restrict our analysis to the homogeneous dynamics and

 © 2010 The American Physical Society

we assume a spatially flat Robertson-Walker background

$$ds^2 = g_{\mu\nu}dx^\mu dx^\nu = -dt^2 + a^2(t)d\vec{x}^2, \tag{2}$$

the variation of the above Lagrangian leads to the following set of independent equations:

$$H^2 = \frac{1}{3\gamma\sigma^2}\left[\frac{\dot{\sigma}^2}{2} + V(\sigma)\right] - 2H\frac{\dot{\sigma}}{\sigma} \tag{3}$$

$$\ddot{\sigma} + 3H\dot{\sigma} + \frac{\dot{\sigma}^2}{\sigma} = -\frac{V_{\mathrm{eff},\sigma}}{1+6\gamma} \tag{4}$$

where we defined $V_{\mathrm{eff},\sigma} = dV/d\sigma - 4V/\sigma$. The left-hand side of Eq. (3) is positive definite or zero whereas the left-hand side of the same equation can also be negative in some regions of the phase-space. As a consequence one has some restrictions on the allowed phase-space. In particular one needs

$$6\gamma - \sqrt{6\gamma(1+6\gamma)} < \frac{\dot{\sigma}}{H\sigma} < 6\gamma + \sqrt{6\gamma(1+6\gamma)} \tag{5}$$

in order for (3) to be well defined.

It is known [13,14] that by a conformal transformation:

$$\tilde{g}_{\mu\nu} = \Omega^2 g_{\mu\nu} \qquad d\tilde{\sigma}^2 = \frac{(1+6\gamma)}{\Omega^2}d\sigma^2 \qquad \tilde{V} = \Omega^{-4}V, \tag{6}$$

where $\Omega^2 = \gamma\sigma^2/\mathrm{M_P}^2$, we can rewrite (up to a boundary term) the action in Eq. (1) as

$$S_E = \int d^4x\sqrt{-\tilde{g}}\left[-\frac{\tilde{g}^{\mu\nu}}{2}\partial_\mu\tilde{\sigma}\partial_\nu\tilde{\sigma} + \frac{\tilde{R}\mathrm{M_P}^2}{2} - \tilde{V}(\tilde{\sigma})\right] \tag{7}$$

and we have introduced a (reduced) Planck mass $\mathrm{M_P}$ ($= (8\pi G)^{-1/2}$ with G the Newton constant).

The variation of Eq. (7) then leads to a set of equations analogous to those obtained from Eq. (1). Let us note that the spectrum of curvature perturbations and the amplitude of gravitational waves obtained are invariant under conformal transformations [15]: it is for this reason that inflationary calculations are often performed in the Einstein frame.

We observe that other important quantities in cosmology are not left invariant under conformal transformation. This is the case for the Hubble parameter H. If we are interested in late time cosmology and use observational data to constrain H in a scalar-tensor theory [11], this should be done for the Hubble parameter in the Jordan frame, which is different from the Hubble parameter in the Einstein frame. To conclude, for us, the Jordan frame is the physical one.

A. Hubble and scalar field flow functions

As emphasized in [12], cosmological linear perturbations depend not only on the derivatives of the Hubble parameter, but also on the derivative of the scalar field itself. It is therefore useful to introduce the hierarchy of scalar field flow functions δ_n ($d\ln|\delta_n|/dN \equiv \delta_{n+1}$ with $n \geq 0$, $\delta_0 \equiv \sigma/\sigma(t_i)$) in addition to ϵ_n ($d\ln|\epsilon_n|/dN \equiv \epsilon_{n+1}$, $\epsilon_0 \equiv H(t_i)/H$) with $n \geq 0$, where t_i is some initial time and $N \equiv \ln\frac{a}{a(t_i)}$ is the number of e-folds. These two hierarchies are related by

$$\epsilon_1 = \frac{\delta_1}{1+\delta_1}\left(\frac{\delta_1}{2\gamma} + 2\delta_1 + \delta_2 - 1\right). \tag{8}$$

The above parameters are related to the Hubble flow functions in the Einstein frame ($\tilde{\epsilon}_i$) by

$$\tilde{\epsilon}_1 = \frac{(1+6\gamma)\delta_1^2}{2\gamma(1+\delta_1)^2} \qquad \tilde{\epsilon}_2 = \frac{2\delta_2}{(1+\delta_1)^2}. \tag{9}$$

These hierarchies arise naturally with the slow-roll (SR) of the inflaton field. Note that in EG the equations governing the dynamics of the scalar and tensor fluctuations during inflation can be written in terms of the Hubble flow function hierarchy. In IG the equivalent set of equations cannot be written only in terms of Hubble flow function hierarchy and the scalar field flow function hierarchy is also needed.

B. Homogeneous dynamics as flow of the Hubble and scalar field flow functions

The homogeneous dynamics of the field-gravity system and the slow-roll conditions for inflation have a peculiar role in the theory of cosmological perturbations since they provide an approximate method to determine the dynamics of these perturbations and compare theoretical models with observations. Exact solutions for such a dynamics can be also found for particular choices of the inflaton potential both in the EG and IG framework. On writing the equations of motion in terms of the SR parameters ϵ_i and δ_i one can easily find a set of these solutions. In EG one has

$$\tilde{\delta}_1^2\frac{\tilde{\sigma}^2}{\mathrm{M_P}^2} = \tilde{\epsilon}_1 \Rightarrow \tilde{\delta}_1 + \tilde{\delta}_2 = \frac{\tilde{\epsilon}_2}{2}, \tag{10}$$

and the Klein-Gordon equation for the scalar field can be rewritten as

$$\tilde{\delta}_2 + \tilde{\delta}_1 - \tilde{\epsilon}_1 + 3 + \frac{\tilde{\delta}_1}{\tilde{\epsilon}_1}\frac{d\ln\tilde{V}}{d\ln\tilde{\sigma}}(3 - \tilde{\epsilon}_1) = 0. \tag{11}$$

From Eqs. (10) and (11) one easily observes that no solution with $\tilde{\delta}_1$ and $\tilde{\epsilon}_1$ simultaneously constant and different from zero exists while a nontrivial solution can be found for the case $\tilde{\epsilon}_2 = 0$, $\tilde{\delta}_1 = \pm\sqrt{\tilde{\epsilon}_1}\mathrm{M_P}/\tilde{\sigma}$ and $\tilde{V} \propto \exp(\sqrt{\tilde{\epsilon}_1}\tilde{\sigma}/\mathrm{M_P})$, namely, the well-known power-law inflationary solution.

In the IG context Eqs. (10) and (11) are replaced by Eq. (8) and

$$\epsilon_1 = \left[3\left(\delta_1 - 4\gamma + \gamma\frac{d\ln V}{d\ln\sigma}\right) + \delta_1\left(6\gamma - \frac{\delta_1}{2}\right)\frac{d\ln V}{d\ln\sigma} + \delta_1(\delta_1 + \delta_2)\right] \times \frac{1}{\delta_1 - 6\gamma}. \quad (12)$$

Despite their quite involved form one can still see that an exact, nontrivial solution exists with $\epsilon_2 = \delta_2 = 0$ when $V = V_0(\sigma/\sigma_0)^n$, that is

$$\delta_1 = -\frac{\gamma(n-4)}{1+\gamma(n+2)}, \qquad \epsilon_1 = \frac{\gamma(n-2)(n-4)}{2+2\gamma(n+2)}. \quad (13)$$

On solving Eqs. (8) and (12) one obtains

$$\delta_1 = 6\gamma \pm \sqrt{6\gamma(1+6\gamma)}, \qquad \epsilon_1 = 3 + 2\delta_1 \quad (14)$$

which are not compatible with phase-space constraints. In Fig. 1 we plotted the behavior of ϵ_1 in (13) on varying γ and n. Decelerated, accelerated and superaccelerated solutions can be found inside the boundaries of phase-space as can be seen in Fig. 1 where the lighter region represents decelerated trajectories ($\epsilon_1 > 1$), the darker area is for superaccelerated solutions ($\epsilon_1 < 0$) and the intermediate grey region represents the accelerated trajectories ($0 < \epsilon_1 < 1$). The outer boundaries of the lighter gray area are those of phase-space and are also those of the region of stability for such exact solutions with respect to homogeneous perturbations. The lines $n = 2$ and $n = 4$ dividing accelerated and superaccelerated trajectories represent the de Sitter solutions. Note finally that the exact solutions with $n \geq 4$ have $\delta_1 \leq 0$ (large field dynamics) while for $n < 4$ one has $\delta_1 > 0$ (small field dynamics).

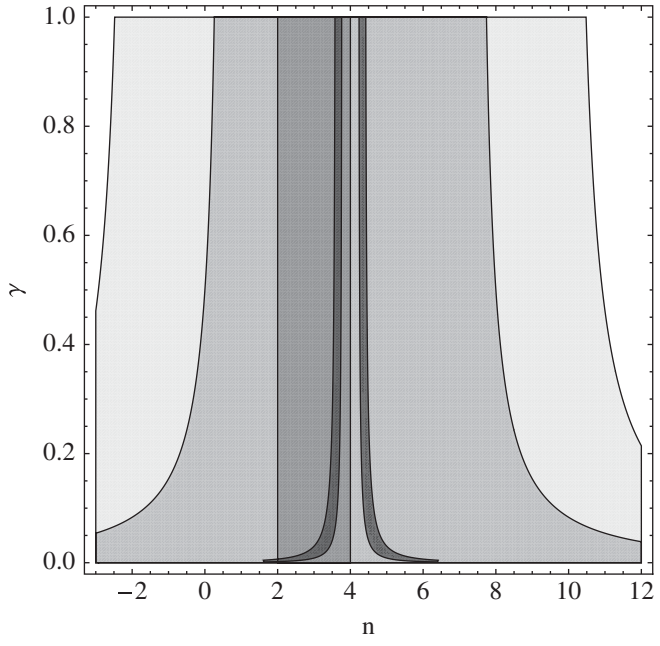

FIG. 1. The figure represents ϵ_1 in (13) as a function of n and γ. The lighter grey region is for $\epsilon_1 > 1$, the darker grey region is for $\epsilon_1 < 0$ and the intermediate grey region is for $0 < \epsilon_1 < 1$. The lines for $n = 2$, 4 represent the de Sitter solutions. The darkest grey areas are the domains allowed by the present experimental constraints (26).

III. COSMOLOGICAL PERTURBATIONS

Scalar curvature perturbations produced by quantum fluctuations of the inflaton during the accelerated stage are described by $\mathcal{R}(x) = -H\delta\sigma(x)/\dot{\sigma}$ in the uniform curvature gauge [16], where $\delta\sigma(x)$ is the scalar inflaton perturbation and is the correct field variable to quantize. The Fourier component $\delta\sigma_k$ ($\mathcal{R}_k = -H\delta\sigma_k/\dot{\sigma}$) of the inflaton fluctuation, in the IG context, has been shown to satisfy the following differential equation [16]:

$$\delta\ddot{\sigma}_k + \left(3H + \frac{\dot{Z}}{Z}\right)\delta\dot{\sigma}_k + \left\{\frac{k^2}{a^2} - \frac{1}{a^3 Z\sigma\delta_1}[a^3 Z(\sigma\delta_1)^{\cdot}]^{\cdot}\right\}\delta\sigma_k = 0 \quad (15)$$

where

$$Z = \frac{H^2\sigma^2(1+6\gamma)}{(\dot{\sigma}+H\sigma)^2} = \frac{1+6\gamma}{(1+\delta_1)^2}. \quad (16)$$

The above equation can be rewritten for $S_k \equiv a\sqrt{Z}\delta\sigma_k$ as

$$\frac{d^2 S_k}{d\eta^2} + [k^2 + M_S^2(\eta)]S_k = 0 \quad (17)$$

where

$$M_S^2(\eta) \equiv -\mathcal{H}^2\left[\delta_1^2 + \delta_2^2 + (3-\epsilon_1)(\delta_1+\delta_2+1) + \delta_2\delta_3 + \frac{\delta_1\delta_2}{1+\delta_1}\left(\epsilon_1 + \delta_1 - 3\delta_2 - \delta_3 + \frac{2\delta_1\delta_2}{1+\delta_1}\right) - 1\right], \quad (18)$$

with η the conformal time ($a(\eta)d\eta \equiv dt$) and $\mathcal{H} \equiv a^{-1}da/d\eta$. Gravitational waves are also produced during inflation. In IG the Fourier modes of tensor perturbations satisfy the following equation:

$$\ddot{h}_{s,k} + (3H + 2H\delta_1)\dot{h}_{s,k} + \frac{k^2}{a^2}h_{s,k} = 0 \quad (19)$$

where $s = +, \times$ denotes the two polarization states. On setting $T_{s,k} \equiv \frac{1}{\sqrt{2}}a\sigma\sqrt{\gamma}h_{s,k}$ the above equation can be rewritten as

$$\frac{d^2 T_{s,k}}{d\eta^2} + [k^2 + M_T^2(\eta)]T_{s,k} = 0, \quad (20)$$

where

$$M_T^2(\eta) \equiv -\mathcal{H}^2[2 - \epsilon_1 + \delta_1(3 + \delta_1 + \delta_2 - \epsilon_1)]. \quad (21)$$

We define the power spectra of scalar curvature perturbations and tensor perturbation as

$$\mathcal{P}_{\mathcal{R}}(k) \equiv \frac{k^3}{2\pi^2}|\mathcal{R}_k|^2 \simeq \mathcal{P}_{\mathcal{R}}(k_*)\left(\frac{k}{k_*}\right)^{n_s-1} \tag{22}$$

and

$$\mathcal{P}_h(k) \equiv \frac{2k^3}{\pi^2}(|h_{+,k}|^2 + |h_{\times,k}|^2) \simeq \mathcal{P}_h(k_*)\left(\frac{k}{k_*}\right)^{n_t} \tag{23}$$

respectively, where k_* is a suitable pivot scale.

A. Exact solutions for $V(\sigma) \propto \sigma^n$

In IG power-law potentials for σ lead to power-law inflation [12] and the spectral index for such background solutions is

$$n_s - 1 = n_t = \frac{2\gamma(n-4)^2}{\gamma(n-4)^2 - 2(6\gamma+1)} \tag{24}$$

and the exact tensor-to-scalar ratio is given by

$$r = \frac{\mathcal{P}_h(k)}{\mathcal{P}_{\mathcal{R}}(k)} = -\frac{8n_t}{1-\frac{n_t}{2}} \tag{25}$$

which agrees with the consistency condition of power-law inflation in EG.

From the most recent compilation of data [17] we obtain the constraint:

$$39 < \frac{6\gamma+1}{\gamma(n-4)^2} < 123 \tag{26}$$

at the 95% confidence level which is independent of γ for γ large.

B. Slow-roll results

For generic potentials the form of the exact solutions of Eqs. (8) and (12) is unknown and one must employ the SR approximation in order to obtain analytical estimates for the spectra of perturbations. In such an approximation Eqs. (3) and (4) become

$$H^2 \simeq \frac{V(\sigma)}{3\gamma\sigma^2} \tag{27}$$

$$3H\dot{\sigma} \simeq -\frac{V_{\mathrm{eff},\sigma}}{1+6\gamma}. \tag{28}$$

On assuming $\delta_i \ll 1$ (and consequently $\epsilon_i \ll 1$) one can thus neglect their variation in time and rely, to first order in the SR parameters, on the results obtained for exact evolution with $\delta_2 \sim \delta_1 \neq 0$. Such an approach leads to the following expressions for the spectra:

$$\mathcal{P}_{\mathcal{R}}(k_*) \simeq \frac{AH_*^2}{4\pi^2(1+6\gamma)\delta_{1*}^2\sigma_*^2} \tag{29}$$

where

$$A = [1 - 2\epsilon_{1*} + C(\delta_{1*} + \delta_{2*} + \epsilon_{1*})], \tag{30}$$

$C = 2\,(2 - \ln 2 - b)$, b is the Euler-Mascheroni constant and

$$\mathcal{P}_h(k_*) \simeq \frac{2(A - C\delta_{2*})H_*^2}{\pi^2\gamma\sigma_*^2}. \tag{31}$$

The spectral indices for the perturbations are

$$n_s - 1 = n_t - 2\delta_2 = -2(\delta_1 + \delta_2 + \epsilon_1), \tag{32}$$

and the tensor-to-scalar ratio is $r = -8n_t$.

In the SR regime the dynamics of the scalar field can be approximated as follows:

$$\delta_1 \equiv \sigma^{-1}\frac{d\sigma}{dN} \simeq -\gamma\sigma\frac{V_{\mathrm{eff},\sigma}}{(1+6\gamma)V}, \tag{33}$$

$$\delta_2 \simeq -\gamma\sigma^2\frac{V_{\mathrm{eff},\sigma\sigma}}{(1+6\gamma)V} + \delta_1\left(\frac{1+6\gamma}{\gamma}\delta_1 - 3\right) \tag{34}$$

and

$$\epsilon_1 \simeq -\delta_1 + \frac{1+6\gamma}{2\gamma}\delta_1^2. \tag{35}$$

Let us note, from Eqs. (33) and (34), that the δ_i are not independent of γ and in the $\gamma \ll 1$ limit $\delta_1 \sim \gamma$ and thus terms proportional to $\delta_1^2/\gamma \sim \delta_i$ should be kept in first-order calculations. Second-order terms in the above expressions are retained in order to better interpolate the regime from large to small γ. On using the above expressions and keeping the first-order contributions one is finally led to [12]

$$n_s - 1 = \frac{2\gamma\sigma_*^2}{1+6\gamma}\left[\frac{V_{\mathrm{eff},\sigma\sigma*}}{V_*} - \frac{3V_{\mathrm{eff},\sigma*}}{\sigma_* V_*} - \frac{3V_{\mathrm{eff},\sigma*}^2}{2V_*^2}\right] \tag{36}$$

and

$$n_t = -\frac{\gamma\sigma_*^2}{1+6\gamma}\frac{V_{\mathrm{eff},\sigma*}^2}{V_*^2} \tag{37}$$

where terms proportional to $V_{\mathrm{eff},\sigma*}^2/V_*^2$ are of first order for $\gamma \ll 1$ and second order for $\gamma \gtrsim 1$.

IV. CONSTRAINTS ON DIFFERENT POTENTIALS

On using the above expressions one can investigate the observational constraints IG inflation imposes on different potentials for the scalar field. In particular we tested the following symmetry-breaking potentials which fix the Planck mass after inflation: a Landau-Ginzburg (LG) potential

$$V_{\mathrm{LG}}(\sigma) = \frac{\mu}{4}(\sigma^2 - \sigma_0^2)^2, \tag{38}$$

a Coleman-Weinberg (CW) type potential

$$V_{\mathrm{CW}}(\sigma) = \frac{\mu}{8}\sigma^4\left(\log\frac{\sigma^4}{\sigma_0^4} - 1\right) + \frac{\mu}{8}\sigma_0^4, \tag{39}$$

a cosine potential (CO)

$$V_{\rm CO}(\sigma) = \Lambda\left[1 + \cos\left(\pi\frac{\sigma}{\sigma_0}\right)\right] \tag{40}$$

and some generalization of the above potentials of the form

$$V_1(\sigma) = \frac{\Lambda}{4n}(\sigma^2 - \sigma_0^2)^{2n} \tag{41}$$

and

$$V_2(\sigma) = \Lambda\left[\left(\frac{\sigma}{\sigma_0}\right)^n - 1\right]^2 \tag{42}$$

with $n > 1$. In particular for our analysis we chose $n = 2$ in the case of (41) and $n = 3/2$ and $n = 5/2$ in the case of (42).

These potentials share a few interesting features: they have a minimum for $\sigma = \sigma_0$ and a relative maximum in $\sigma = 0$, $V(\sigma) \geq 0$ and all of them allow both small and large field inflation. We further note that we have included the CO potential even if it agrees to lowest order with the LG potential on expanding around σ_0. Nonetheless it leads to slightly different results because of higher-order effects. On assuming that the pivot mode exits the horizon from 50 to 70 e-folds (N_*) before inflation ends, one can compare theoretical predictions for $n_s - 1$ and r with WMAP5 + BAO + SN observations [18] for different choices of γ.

In Figs. 2 and 3 (where the outer border of the lighter grey region represents the 68% confidence level and the border of the dark grey region the 95% confidence level) we plotted the trajectories of (n_s, r) for $N_* = 50$ (line with empty markers) and $N_* = 70$ (line with filled markers) as a function of γ. The markers on the trajectories represent particular choices of $L_\gamma \equiv \log\gamma$ and each trajectory splits into a dotted line, for the SF regime, and a solid line for the LF regime predictions. Note that the transition between the two regimes simply occurs in the $\gamma \to 0$ limit. The dashed line in each figure represents the exact consistency condition (25) which is $rn_s = 3r + 16n_s - 16$.

Potentials (38) and (39) do not constrain γ in the LF regime but they need $L_\gamma < -4$ for successful inflation in the SF case. Indeed from Fig. 2 one can see that the markers for $L_\gamma = 3$ lie outside the 68% confidence lever region. For different choices of the potential we observe that both the SF and the LF regimes impose limits on γ (apart from the potential in ((41) with $n = 2$) which is not compatible with observations independently of γ). In particular for $50 \leq N_* \leq 70$, $L_\gamma \lesssim -4$ is needed in the SF case and $L_\gamma \lesssim -2$ in the LF case.

One can estimate the coordinate of some relevant points of the trajectories in Figs. 2 and 3 as functions of N_*. On observing that the dynamics of σ during inflation is strongly dependent on the value of γ (33) and (34) then, in the $\gamma \ll 1$ limit, one can safely assume that $|\sigma_* - \sigma_0|/\sigma_0 \ll 1$. In order to relate σ_* and N_* one needs to integrate the SR condition (33) by parts:

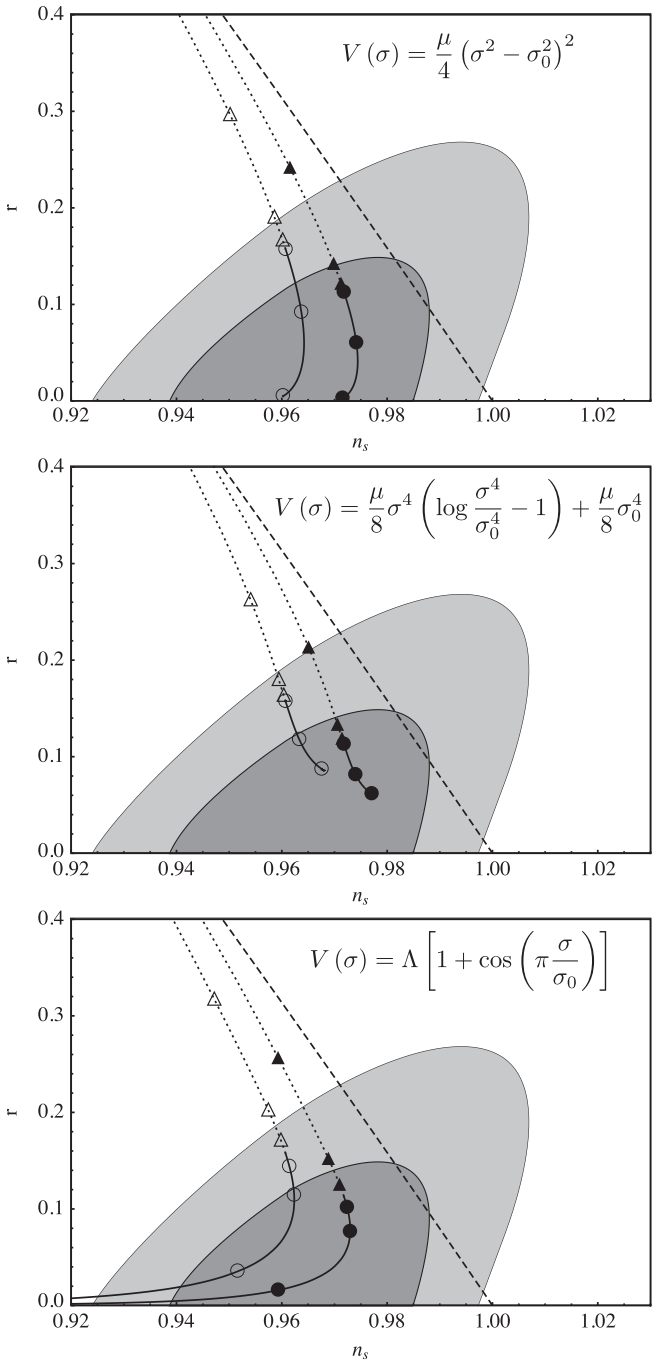

FIG. 2. The trajectories of the vector (n_s, r) on varying γ and potentials (38)–(40). For (38) and (39) the markers represent $L_\gamma = -5, -4, -3$ in the SF and $L_\gamma = -7, -3, +1$ in the LF regimes. For (40) the markers are for $L_\gamma = -5, -4, -3$ both in the SF and in the LF regimes. The order of the markers is such that dotted and continuous lines join for $L_\gamma \to -\infty$. The same order is followed in Fig. 3.

$$\int_{\sigma_*}^{\sigma_0} \frac{1 + \gamma(n(\sigma) + 2)}{\gamma\sigma(4 - n(\sigma))} d\sigma = \int_0^{N_*} dN = N_* \tag{43}$$

where $n(\sigma) \equiv d\log V(\sigma)/d\log\sigma$ and we approximate $\sigma_{\rm end}$

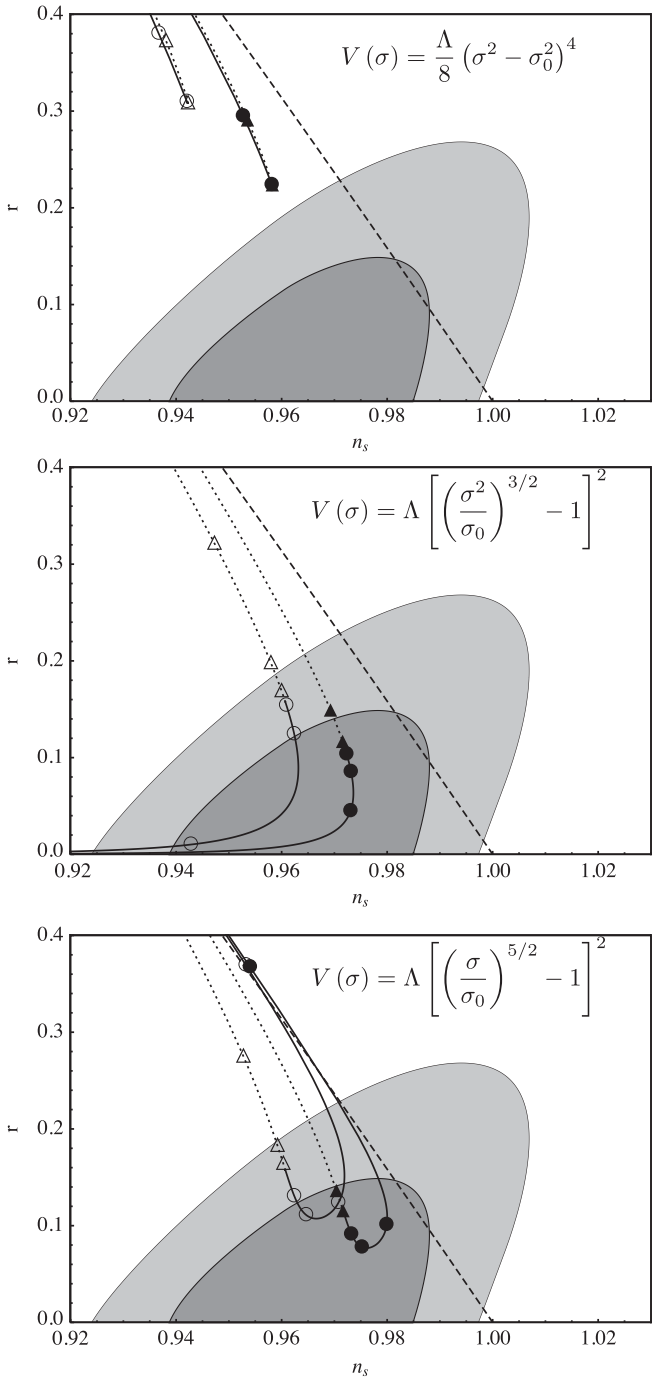

FIG. 3. The trajectories of the vector (n_s, r) on varying γ for potential (41) with $n = 2$ and potential (42) with $n = 3/2$ and $n = 5/2$ respectively. In the top figure, for potential (41) with $n = 2$, the markers represent $L_\gamma = -5, -3$ both in the SF and in the LF regime. In the middle figure, for potential (42) and $n = 3/2$, the markers are $L_\gamma = -5, -4, -3$ in the SF regime and $L_\gamma = -6, -4, -2$ in the LF regime. In the lowest figure, for potential (42) and $n = 5/2$, the markers are $L_\gamma = -5, -4, -3$ in the SF regime and $L_\gamma = -3.6, -2.8, -2.0, -1.2$ in the LF regime.

(the value of σ when inflation ends) with σ_0 since $\sigma_{\rm end} = \sigma_0(1 \pm \mathcal{O}(\gamma))$. In general, the integral on the left-hand side of Eq. (43) cannot be solved exactly for any potential $V(\sigma)$, and even when it is possible, one further needs to invert the result in order to obtain $\sigma_* = \sigma(N_*)$ which is often a difficult task. For $\gamma \ll 1$, however, simplifications occur and a double series expansion in γ and $(\sigma_* - \sigma_0)/\sigma_0$ leads to good predictions. In particular one finds $\sigma(N_*) \simeq \sigma_0(1 - 2\sqrt{\gamma N_*})$, $n_s \simeq 1 - 2/N_*$ and $r \simeq 8/N_*$ for the potentials (38) and (39) and for (42) with $n = 3/2$ and $n = 5/2$, in agreement with the numerical result [19]. Potential (41) with $n = 2$ is quite different and leads to $\sigma(N_*) \simeq \sigma_0(1 - 2\sqrt{2\gamma N_*})$, $n_s \simeq 1 - 3/N_*$ and $r \simeq 16/N_*$ for $\gamma \ll 1$. Thus, depending on the shape of the potential, for small γ, predictions can be incompatible with observations for a 50–70 e-fold inflation. For γ large inflation takes place in the LF regime and one can still invert Eq. (43) on assuming $\sigma_* \gg \sigma_0$ and series expanding γ^{-1} and $(\sigma_* - \sigma_0)/\sigma_*$ (around zero). One obtains $n_s \simeq 1 - 2/N_*$ and $r \simeq 12/N_*^2$ for potential (38) and $n_s \simeq 1 - 1.5/N_*$ and $r \simeq 4/N_*$ for potential (39). In both cases predictions agree with observations but the results are quite different.

Furthermore in Figs. 4 and 5 we have plotted the observational constraints on the potentials coming from the amplitude of the scalar perturbations

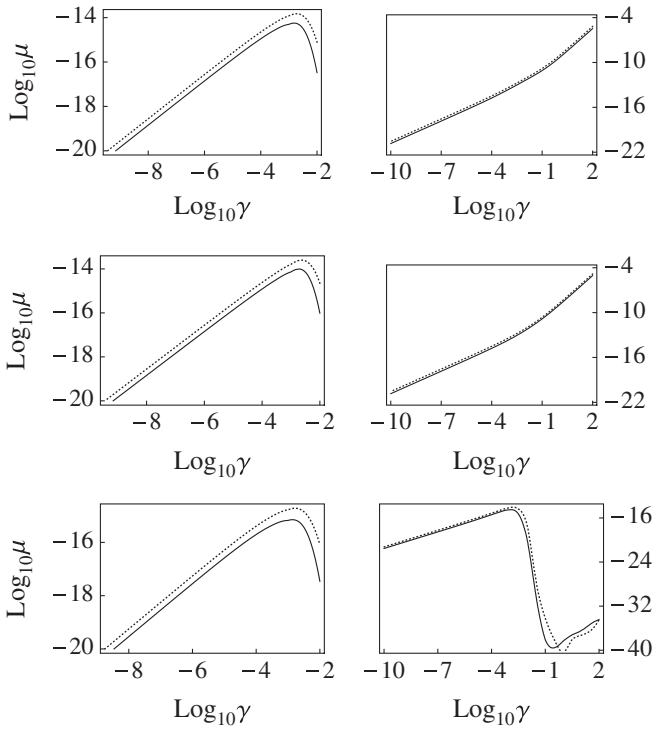

FIG. 4. Constraints on μ from the amplitude of the scalar perturbations (44) for potentials (38)–(40) respectively, where $\mu \equiv \Lambda/\sigma_0^4$ for (40). The dotted line is for $N_* = 50$ and the solid line is for $N_* = 70$ e-folds. The plots on the left refer to the SF case and the ones on the right to the LF.

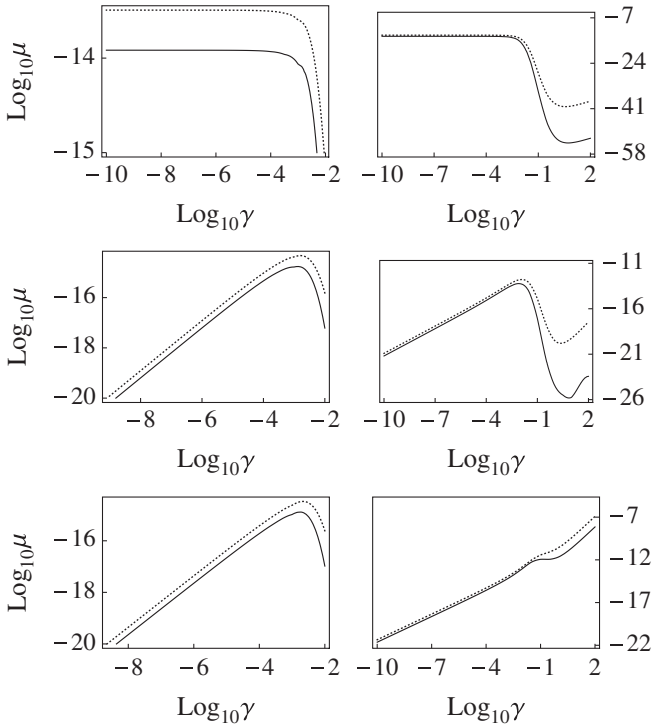

FIG. 5. Constraints on μ from the amplitude of the scalar perturbations (44) for potentials (41) with $n = 2$ and (42) with $n = 3/2$ and $n = 5/2$ respectively, where $\mu \equiv \Lambda\sigma_0^4$ for (41) and $\mu \equiv \Lambda/\sigma_0^4$ for (42). The dotted line is for $N_* = 50$ and the solid line is for $N_* = 70$ e-folds. The plots on the left refer to the SF case and the ones on the right to the LF.

$$P_{\mathcal{R}}(k^*) = (2.445 \pm 0.096) \times 10^{-9} \tag{44}$$

derived from WMAP5 + BAO + SN [18]. The constraints on μ, where $\mu \equiv \Lambda/\sigma_0^4$ in the case of (40) and (42) and $\mu = \Lambda\sigma_0^4$ in the case of (41), are plotted for varying L_γ and assuming $N_* = 50$ (dotted lines) and $N_* = 70$ (solid lines).

V. COHERENT OSCILLATIONS

In general, in order to avoid never-ending inflation, it is necessary the inflationary potential has a minimum in which case the accelerated epoch is followed by a stage in which the inflaton oscillates about it. In realistic models of inflation it is usually assumed that during this phase the inflaton decays into ordinary matter. This regime of coherent oscillations was studied in the context of EG in Ref. [20] through the use of a time-averaging procedure which relied on the fact that the frequency of oscillation of the scalar field is much larger than the Hubble parameter.

We have studied the coherent oscillations of the scalar field in the context of IG finding the following solutions [12]:

$$\sigma(t) = \sigma_0 + \frac{2}{t}\sqrt{\frac{\gamma}{3\mu}}\sin(\omega_0 t) + \mathcal{O}\left(\frac{1}{t^2}\right) \tag{45}$$

$$H(t) \simeq \frac{2}{3t}\left[1 - \sqrt{\frac{6\gamma}{1+6\gamma}}\cos(\omega_0 t)\right] + \mathcal{O}\left(\frac{1}{t^2}\right) \tag{46}$$

for a potential which can be approximated

$$V(\sigma) \simeq \frac{m^2}{2}(\sigma - \sigma_0)^2 \tag{47}$$

around the minimum. The frequency of the oscillations is given by:

$$\omega_0 = \sqrt{\frac{m^2}{1+6\gamma}}. \tag{48}$$

A. MSA method

The method we employ relies on the assumption that, during the coherent oscillations phase, two different time scales enter the evolution of the field: the frequency of the oscillations around the minimum and the damping rate of their amplitude, the former being much bigger than the latter. This assumption will be verified at the end of the calculations.

On using Eqs. (3) and (4) one can write the second-order equation which governs the homogeneous evolution of the scalar field in the absence of matter. For a generic potential $V(\sigma)$ one finds

$$\ddot{\sigma} + \frac{1}{1+6\gamma}\left(\frac{dV(\sigma)}{d\sigma} - 4\frac{V(\sigma)}{\sigma}\right) - 2\frac{\dot{\sigma}^2}{\sigma} + \frac{\dot{\sigma}}{\sigma}\sqrt{\frac{3}{2\gamma}[2V(\sigma) + (1+6\gamma)\dot{\sigma}^2]} = 0. \tag{49}$$

If the potential has a minimum for $\sigma = \sigma_0$ then the equation governing the dynamics of $\delta\sigma = \sigma - \sigma_0$ can be expanded around it up to second order in $\delta\sigma/\sigma_0$ obtaining

$$\delta\ddot{\sigma} + \omega_0^2\delta\sigma + \frac{\bar{n} - 4m^2/\sigma_0}{2(1+6\gamma)}\delta\sigma^2 - 2\frac{\delta\dot{\sigma}^2}{\sigma_0} + \frac{\delta\dot{\sigma}}{\sigma_0}\sqrt{\frac{3(1+6\gamma)}{2\gamma}[\omega_0^2\delta\sigma^2 + \delta\dot{\sigma}^2]} = 0 \tag{50}$$

and for small displacements around the minimum of the potential one has

$$V(\sigma) \equiv \frac{m^2}{2}\delta\sigma^2 + \mathcal{O}(\delta\sigma^3), \tag{51}$$

$$\frac{dV(\sigma)}{d\sigma} \equiv m^2\delta\sigma + \frac{\bar{n}}{2}\delta\sigma^2 + \mathcal{O}(\delta\sigma^3) \tag{52}$$

where $[\bar{n}] = [m]$. The effect of the friction terms in (4) ensures that $\delta\sigma/\sigma_0 \ll 1$ for some time $\bar{t}$ and consequently the second-order equation is a good approximation for $t > \bar{t}$. On examining Eq. (50) we observe that second-order contributions are responsible for the "slow" time scale evolution while the "fast" dynamics is that of an harmonic

oscillator with frequency ω_0. On explicitly taking into account the two time scales, we look for a solution in the form

$$\delta\sigma = \delta\sigma(t,\tau) = \delta\sigma_0(t,\tau) + \epsilon\delta\sigma_1(t,\tau) + \mathcal{O}(\epsilon^2) \quad (53)$$

with $\tau \equiv \epsilon t$. On replacing $\delta\sigma/\sigma_0 \rightarrow \epsilon\delta\sigma/\sigma_0$ in (50) one is finally led to the set of partial differential equations for $\delta\sigma_0$ and $\delta\sigma_1$:

$$\delta\ddot{\sigma}_0 + \omega_0^2\delta\sigma_0 = 0 \quad (54)$$

$$\delta\ddot{\sigma}_1 + \omega_0^2\delta\sigma_1 = -2\frac{\partial^2\delta\sigma_0}{\partial t\partial\tau} - \frac{\bar{n} - 4m^2/\sigma_0}{2(1+6\gamma)}\delta\sigma_0^2 + 2\frac{\delta\dot{\sigma}_0{}^2}{\sigma_0} - \frac{\delta\dot{\sigma}_0}{\sigma_0} \times\sqrt{\frac{3(1+6\gamma)}{2\gamma}}[\omega_0^2\delta\sigma_0^2 + \delta\dot{\sigma}_0{}^2]. \quad (55)$$

The standard MSA method consists in writing the general solution for (54) as

$$\delta\sigma_0 = A^*(\tau)e^{i\omega_0 t} + \text{c.c.} \quad (56)$$

and determining $A(\tau)$ by requiring the cancellation of secular terms in the next-to-leading-order Eq. (55) [see [21] for details]. From this procedure one obtains the following differential equation for $A(\tau)$

$$\frac{dA}{d\tau} + \sqrt{\frac{3(1+6\gamma)}{2\gamma}}\frac{\omega_0}{\sigma_0}|A|A = 0 \quad (57)$$

and on setting $A(\tau) = R(\tau)e^{i\theta(\tau)}$ one finds $\theta(\tau) = \theta_0$ and

$$R(\tau) = \frac{R_0}{1 + \frac{R_0}{\sigma_0}\sqrt{\frac{3(1+6\gamma)}{2\gamma}}\omega_0\tau} = \sigma_0\frac{fr}{1 + r\omega_0 t} \quad (58)$$

where

$$f \equiv \sqrt{\frac{2\gamma}{3(1+6\gamma)}}, \qquad r \equiv \frac{\Omega_0}{\omega_0} = \frac{R_0}{f\sigma_0} \quad (59)$$

and $\Omega_0 = R_0\sqrt{3\mu/\gamma}$ is the inverse of the slow time scale. Let us note that the ratio r between the two time scales depends on the ratio R_0/σ_0 and on f, where f is a function of γ having values between 0 and $\sqrt{1/3}$. On setting $\sigma_0 = \mathrm{M_P}/\sqrt{\gamma}$ one finds

$$r = \sqrt{\frac{1+6\gamma}{2}}\frac{R_0}{\mathrm{M_P}} \ll 1 \Rightarrow \frac{R_0}{\mathrm{M_P}} \ll \sqrt{\frac{2}{1+6\gamma}} \quad (60)$$

which is the condition for the MSA method to well approximate the dynamics. The general solution for (50) turns out to be

$$\delta\sigma = \sigma_0\frac{2fr}{1 + r\omega_0 t}\cos(\omega_0 t + \theta_0), \quad (61)$$

and the constants R_0 and θ_0 are related to the initial conditions of the second-order Eq. (50).

The MSA method is generally applied to first order, nonetheless we found numerically that our results were significantly improved once the second-order contributions on the right-hand side of Eq. (55) were taken into account. These terms slowly vary in time and give a second-order shift to the center of the oscillations which has to be added to the right-hand side of (61)

$$\Delta_{\bar{n}} = |A|^2\left(\frac{8}{\sigma_0} - \frac{\bar{n}}{m^2}\right) \quad (62)$$

and plays a crucial role in the calculations of the next sections. In particular one has $\bar{n}_{\mathrm{LG}} = 6\mu\sigma_0$ and $\bar{n}_{\mathrm{CW}} = 10\mu\sigma_0$ and $m^2 = 2\mu\sigma_0^2$ for both LG and CW potentials.

B. Equation of state

A first application of the above results is the calculation of the averaged equation of state of the scalar field during the oscillatory regime. It is known (and can be shown with the same technique we are employing) that the averaged massive oscillations of a scalar field in EG are equivalent to a fluid with null equation of state in agreement with [20]. On the other hand, in IG, for the potentials we are considering, oscillations around the minimum are still massive but the results are somewhat different.

The definition of energy density and pressure for a scalar field in IG can be given [11] further in the EG form:

$$\rho_\sigma \equiv 3\gamma\sigma_0^2H^2, \qquad P_\sigma \equiv -2\gamma\sigma_0^2\left(\dot{H} + \frac{3}{2}H^2\right). \quad (63)$$

With the above definitions continuity equation is satisfied. At the end of inflation the expressions on the right-hand side of (63) are oscillating functions and one may define the averaged quantities $\langle\rho_\sigma\rangle$ and $\langle P_\sigma\rangle$ where

$$\langle A(t)\rangle = \frac{1}{T}\int_{t-T/2}^{t+T/2} A(t')dt' \quad (64)$$

and $T = 2\pi/\omega_0$ is the period of oscillation. Further one may define the averaged equation of state by

$$w \equiv \frac{\langle P_\sigma\rangle}{\langle\rho_\sigma\rangle}. \quad (65)$$

On averaging the expressions (63), using the solution for $\delta\sigma + \Delta_{\bar{n}}$ and keeping contributions up to the second order in $R(t)/\sigma_0 \ll 1$ one finds

$$\langle\rho_\sigma\rangle = (1+9\gamma)\langle\delta\dot{\sigma}^2\rangle \quad (66)$$

and

$$\langle P_\sigma\rangle = -[3\gamma + \sqrt{6\gamma(1+6\gamma)}\sin\omega_0 t]\langle\delta\dot{\sigma}^2\rangle \quad (67)$$

where

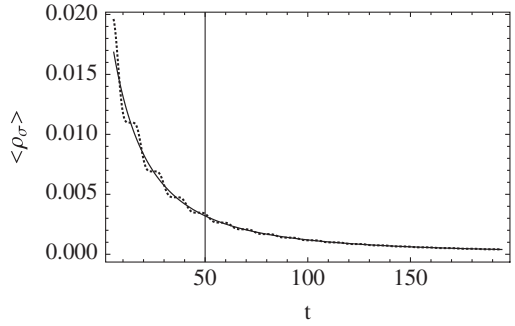

FIG. 6. An example of the average value of the energy density of the scalar field, as given in (63), for (38), $\gamma = 10$, $\mu = 10$ calculated exactly (dotted line) and with MSA in (66) (solid line). The plot shows good agreement between exact and approximate solutions.

$$\langle \delta\dot{\sigma}^2 \rangle = 4\omega_0\sigma_0 \frac{f^2 r^2}{(1 + r\omega_0 t)^2} \tag{68}$$

leading to

$$\langle w \rangle = -\frac{3\gamma}{1 + 9\gamma}. \tag{69}$$

In Fig. 6 we plot the average $\langle \rho_\sigma \rangle$ calculated numerically (dotted line) and analytically as in Eq. (66) for the potential (38) with $\gamma = 10$ and $\mu = 10$. The plot shows that multiple scale predictions agree well with the corresponding exact quantities. Good agreement between the analytical predictions of Eq. (67) and the numerical solutions is also evident in Fig. 7 for the potential (38) with $\gamma = 10$ and $\mu = 10$. In this plot the dotted line represents both the numerical (exact) expression and its analytical approximation (67), since both coincide within the resolution of the figure, the solid and the dashed lines are, respectively, the

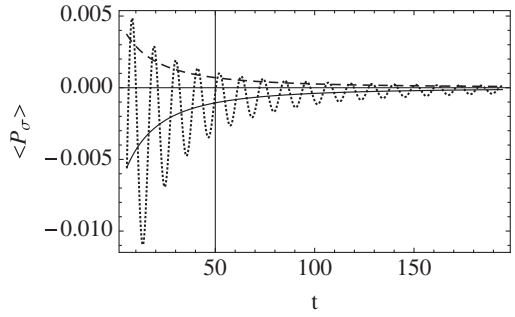

FIG. 7. In the above plot examples are given of the average pressure versus time for the potential (38) with $\gamma = 10$ and $\mu = 10$. The dotted line corresponds to both the average value of the pressure of the scalar field as defined in (63) calculated exactly (numerically) and the plot of (67), since both coincide within the resolution of the figure. The solid line is the average of (67) and the dashed line is the average of the pressure calculated without considering the correction term (62). The plot shows good agreement between exact and approximate values.

average of $\langle P_\sigma \rangle$ with and without adding the improvement (62) to (61).

In contrast with EG, in IG the averaged equation of state defined by (65) does not lead to the correct averaged expansion, as can be directly verified on using (46). The averaged Hubble parameter is simply $\langle H(t) \rangle \simeq 2/(3t)$, namely, that of a matter dominated Universe, independently of the equation of state (69). This difference is a consequence of the fact that in EG one can verify that $\langle H_{(\mathrm{EG})} \rangle \simeq \sqrt{\langle H^2_{(\mathrm{EG})} \rangle}$ whereas in IG such a relation does not hold.

VI. REHEATING

On assuming that the inflaton field is coupled to ordinary matter, then at the end of inflation such a scalar field can decay into lighter particles losing its energy density and eventually reheating the Universe. Such a process has been traditionally described through a phenomenological decay width Γ which enters the equation for the scalar field as an additional friction term:

$$\ddot{\sigma} + (3H + \Gamma)\dot{\sigma} + V_{,\sigma} - 6\gamma\left(H^2 + \frac{\ddot{a}}{a}\right)\sigma = 0. \tag{70}$$

On requiring that the newly added friction term does not affect the Einstein equations (the Bianchi identities must still hold) one observes that the continuity equation for radiation should also be modified as

$$\dot{\rho}_R = -3H(\rho_R + P_R) + \Gamma\dot{\sigma}^2. \tag{71}$$

The system of Eqs. (70) and (71) can be solved numerically but analytical solutions are needed to estimate the reheating temperature of the relativistic particle fluid. In order to simulate the energy transfer from the inflaton to radiation and estimate the reheating temperature, we need the definition of the energy density and pressure of the scalar field. In the presence of relativistic matter the expressions for the energy density and pressure of the scalar field, Eqs. (63), must be modified as

$$\rho_\sigma = 3\gamma\sigma_0^2 H^2 - \rho_R \tag{72}$$

$$P_\sigma = -2\gamma\sigma_0^2\left(\dot{H} + \frac{3}{2}H^2\right) - \rho_R - P_R; \tag{73}$$

with these definitions the continuity equation for ρ_σ, P_σ is still automatically conserved and the introduction of the decay-rate Γ leads to

$$\dot{\rho}_\sigma = -3H(\rho_\sigma + P_\sigma) - \Gamma\dot{\sigma}^2. \tag{74}$$

Let us note that Eqs. (71) and (74) are formally the same as in EG, but they lead to different predictions.

The reheating temperature can be estimated on considering the evolution of ρ_R and $\langle \rho_\sigma \rangle$ as $T_{\mathrm{RH}} \sim \rho_R^{1/4}$ when $\rho_R \gtrsim \langle \rho_\sigma \rangle$. In EG one can naively observe that this hap-

pens when $3H \sim \Gamma$ and one finds the well-known estimate $T_{\mathrm{RH}}^{(\mathrm{EG})} \sim \sqrt{\Gamma \mathrm{M_P}}$.

The continuity equations for ρ_R and $\langle \rho_\sigma \rangle$ can be estimated by the MSA method. Starting from the modified equation for σ

$$\ddot{\sigma} + \frac{1}{1+6\gamma}\left(\frac{dV(\sigma)}{d\sigma} - 4\frac{V(\sigma)}{\sigma}\right) - 2\frac{\dot{\sigma}^2}{\sigma} + \frac{\dot{\sigma}}{\sigma}\sqrt{\frac{3}{2\gamma}[2V(\sigma) + (1+6\gamma)\dot{\sigma}^2) + 2\rho_R]} + \frac{\Gamma}{1+6\gamma}\dot{\sigma} = 0,$$

one can expand to second order in $\delta\sigma \equiv \sigma - \sigma_0$ and consider $\rho_R \sim V(\sigma) \sim \delta\dot{\sigma}^2$ and $\Gamma \sim H \sim \delta\dot{\sigma}/\sigma_0$. These assumptions are reasonable for the regime we are considering [22], nonetheless they will be checked numerically. On expanding one finds

$$\delta\ddot{\sigma} + \omega_0^2\delta\sigma + \frac{\bar{n} - 4m^2/\sigma_0}{2(1+6\gamma)}\delta\sigma^2 - 2\frac{\delta\dot{\sigma}^2}{\sigma_0} + \frac{\Gamma}{1+6\gamma}\delta\dot{\sigma} + \frac{\delta\dot{\sigma}}{\sigma_0}\sqrt{\frac{3(1+6\gamma)}{2\gamma}\left[\omega_0^2\delta\sigma^2 + \delta\dot{\sigma}^2 + \frac{2\rho_R}{1+6\gamma}\right]} = 0. \tag{75}$$

If the fast time evolution is still determined by the leading-order terms $\delta\ddot{\sigma}_0 + \omega_0^2\delta\sigma_0 = 0$ then, on setting $\delta\sigma_0 = A(\tau)y(t)$ and requiring the cancellation of singularities, one obtains the differential equation

$$2\dot{A} + \frac{\Gamma}{1+6\gamma}A + 3\sqrt{\frac{\rho_R + (1+6\gamma)A^2E_F}{3\gamma\sigma_0^2}}A = 0 \tag{76}$$

where $E_F \equiv \frac{1}{2}\dot{y}^2 + \frac{\omega_0^2}{2}y^2$. On then keeping the second-order contributions in the continuity Eq. (71) and averaging over fast oscillations of y one then finds

$$\dot{\rho}_R - \Gamma A E_F + 4\sqrt{\frac{\rho_R + (1+6\gamma)A^2E_F}{3\gamma\sigma_0^2}}\rho_R = 0 \tag{77}$$

where $\langle \delta\dot{\sigma}^2 \rangle = A^2E_F$. On noting that

$$\sqrt{\frac{\rho_R + (1+6\gamma)A^2E_F}{3\gamma\sigma_0^2}} = \langle H \rangle \tag{78}$$

and

$$\langle \rho_\sigma \rangle = A^2E_F(1+9\gamma) \tag{79}$$

where H and ρ_σ are expanded to the second order, one is finally led to the system of averaged equations

$$\dot{\rho}_R = -4\langle H \rangle \rho_R + \frac{\Gamma}{1+9\gamma}\langle \rho_\sigma \rangle \tag{80}$$

$$\langle \dot{\rho}_\sigma \rangle = -3\langle H \rangle \langle \rho_\sigma \rangle - \frac{\Gamma}{1+6\gamma}\langle \rho_\sigma \rangle \tag{81}$$

$$\langle H \rangle = \sqrt{\frac{\rho_R + \frac{1+6\gamma}{1+9\gamma}\langle \rho_\sigma \rangle}{3\gamma\sigma_0^2}} \tag{82}$$

with $\frac{d\langle \rho_\sigma \rangle}{dt} = \langle \dot{\rho}_\sigma \rangle$.

On comparing the above equations with those arising in EG for a massive inflaton we observe that averaged energy transfer is less efficient because of the factors $(1+9\gamma)^{-1}$ and $(1+6\gamma)^{-1}$ in (80) and (81).

In Figs. 8 we have plotted the comparison of the energy transfer obtained numerically on solving (70) and (71) with that calculated by numerically solving the averaged Eqs. (80)–(82). The continuous line is

$$\Omega_\sigma \equiv \frac{\langle \rho_\sigma \rangle}{\rho_R + \langle \rho_\sigma \rangle}, \tag{83}$$

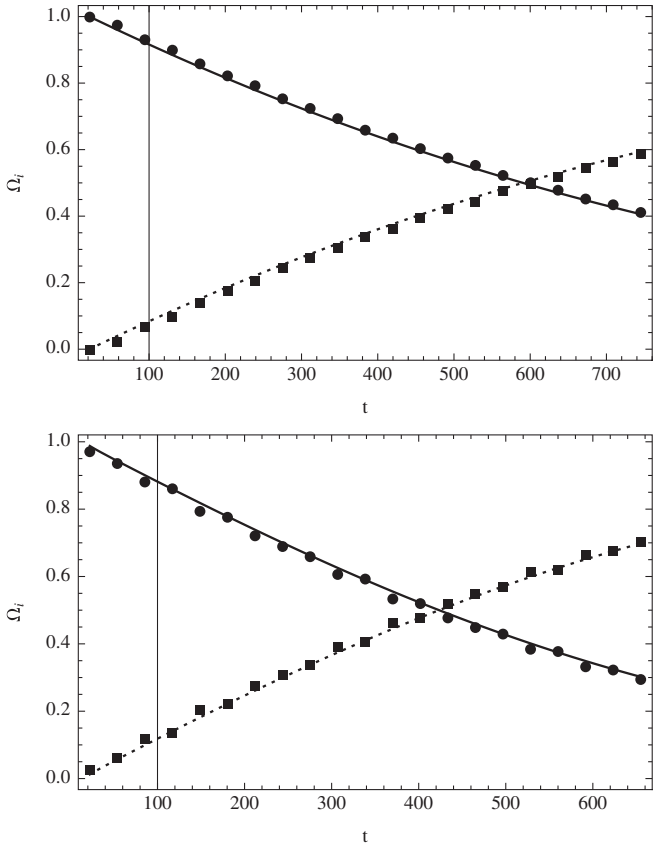

FIG. 8. In these figures the solid line is for (83) and the dotted line is for (84) where both are calculated as numerical solutions to Eqs. (80)–(82). Circles and squares represent the same quantities evaluated on solving (75) and (71) and then averaging the definition (72). The figure on top is for $\Gamma = 2 \cdot 10^{-3}\mathrm{M_P}$, $\gamma = 10^{-2}$ and the lower figure is for $\Gamma = 2 \cdot 10^{-1}\mathrm{M_P}$, $\gamma = 10$. Both situations are described well by the approximation scheme used. Time evolution is expressed in $\mathrm{M_P}^{-1}$ units.

and the dashed line is

$$\Omega_R \equiv \frac{\rho_R}{\rho_R + \langle\rho_\sigma\rangle}. \tag{84}$$

The round dots plot Ω_σ and the square dots plot Ω_R where the averages are calculated numerically from the exact numerical solutions by using (64). In particular the plots are obtained on setting $\gamma\sigma_0^2 = \mathrm{M_P}^2$ for $\Gamma = 2\cdot 10^{-3}\mathrm{M_P}$, $\gamma = 10^{-2}$ (figure on top) and $\Gamma = 2\cdot 10^{-1}\mathrm{M_P}$, $\gamma = 10$ (lower figure). In both regimes Eqs. (80)–(82) describe well the exact dynamics and, qualitatively, it appears that particle production is enhanced for γ small (when the EG predictions are recovered).

A. The reheating temperature

We are interested in estimating the energy density of radiation when it starts dominating over the scalar field. At the onset of this stage the averaged Friedmann Eq. (82) can be approximated by

$$\langle H\rangle \simeq \sqrt{\frac{\frac{1+6\gamma}{1+9\gamma}\langle\rho_\sigma\rangle}{3\gamma\sigma_0^2}} \tag{85}$$

and the system of Eqs. (80), (81), and (85) can be solved analytically.

On defining $\tilde{\rho}_\sigma \equiv \frac{1+6\gamma}{1+9\gamma}\langle\rho_\sigma\rangle$ and $\tilde{\Gamma} = (1+6\gamma)^{-1}\Gamma$ Eqs. (80) and (81) take the form

$$\frac{d\rho_R}{dt} = -4\sqrt{\frac{\tilde{\rho}_\sigma}{3\gamma\sigma_0^2}}\rho_R + \tilde{\Gamma}\tilde{\rho}_\sigma \tag{86}$$

$$\frac{d\tilde{\rho}_\sigma}{dt} = -3\sqrt{\frac{\tilde{\rho}_\sigma}{3\gamma\sigma_0^2}}\tilde{\rho}_\sigma - \tilde{\Gamma}\tilde{\rho}_\sigma \tag{87}$$

which is exactly the form one has in EG for a minimally coupled, massive scalar field. As a consequence of this formal analogy one expects $\tilde{\rho}_\sigma \sim \rho_R$ when $\sqrt{3\tilde{\rho}_\sigma} \simeq \Gamma\mathrm{M_P}/(1+6\gamma)$ or equivalently $t \sim \tilde{\Gamma}^{-1}$.

Equation (87) can be solved easily and leads to

$$\langle\rho_\sigma\rangle = \frac{\gamma\sigma_0^2}{3}\frac{1+9\gamma}{(1+6\gamma)^3}\frac{\Gamma^2}{[C_0\exp(\frac{\Gamma}{2(1+6\gamma)}t)-1]^2} \tag{88}$$

where C_0 is an integration constant and we assumed that the energy transfer begins at $t = 0$. On setting

$$C_0 = 1 + \frac{\Gamma}{3}\sqrt{\frac{3\gamma\sigma_0^2}{\langle\rho_\sigma\rangle_0}\cdot\frac{1+9\gamma}{(1+6\gamma)^3}} \tag{89}$$

one can explicitly obtain the dependence of C_0 on the initial condition for the energy density $\langle\rho_\sigma\rangle_0$. Further Eq. (86) can also be solved and on setting $\rho_R(0) = 0$ one obtains

$$\rho_R = \frac{\Gamma^2\gamma\sigma_0^2}{20(1+6\gamma)^2}\frac{[(\mathrm{e}^{((\Gamma t)/(2(1+6\gamma)))}B_0 - 1)^{5/3}(3\mathrm{e}^{((\Gamma t)/(2(1+6\gamma)))}B_0 + 5) - b_0^{5/3}\mathrm{e}^{((4\Gamma t)/(3(1+6\gamma)))}(3b_0+8)]}{(\mathrm{e}^{((\Gamma t)/(2(1+6\gamma)))}B_0 - 1)^{8/3}} \tag{90}$$

where

$$B_0 = 1 + \Gamma\sqrt{\frac{\gamma\sigma_0^2}{3\langle\rho_\sigma\rangle_0}\cdot\frac{1+9\gamma}{(1+6\gamma)^2}} \tag{91}$$

and $b_0 = B_0 - 1$. If one now considers b_0 and sets $\gamma\sigma_0^2 = \mathrm{M_P}^2$ then

$$b_0 = \frac{\Gamma\mathrm{M_P}}{\langle\rho_\sigma\rangle_0^{1/2}}\sqrt{\frac{1+9\gamma}{3(1+6\gamma)^3}} \simeq \mathcal{O}\left(\frac{\Gamma}{\langle H\rangle_0}\right) \ll 1 \tag{92}$$

since it is generally assumed that $\Gamma \ll \langle H_0\rangle$, where $\langle H_0\rangle$ is the average value of H at the beginning of reheating. The expression (90) then simplifies and becomes

$$\rho_R \simeq \frac{\Gamma^2\gamma\sigma_0^2}{20(1+6\gamma)^2}\cdot\frac{3\mathrm{e}^{((\Gamma t)/(2(1+6\gamma)))}+5}{\mathrm{e}^{((\Gamma t)/(2(1+6\gamma)))}-1}; \tag{93}$$

and on evaluating it for $t \sim (1+6\gamma)\Gamma^{-1}$ one finally obtains:

$$\rho_R((1+6\gamma)\Gamma^{-1}) \simeq \frac{3\Gamma^2\mathrm{M_P}^2}{(1+6\gamma)^2}. \tag{94}$$

On performing the same calculations as above in EG one obtains

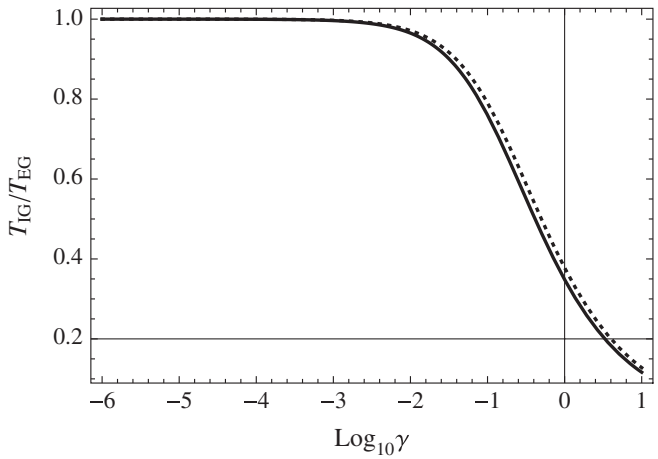

FIG. 9. The continuous line represents the ratio (96) evaluated numerically on using the exact equations for the time of equality t_*. The dotted line is the analytical estimate of the same temperature ratio obtained from (94) and (95) as $T_{\mathrm{reh}}^{(\mathrm{IG})}/T_{\mathrm{reh}}^{(\mathrm{EG})} = (1+6\gamma)^{-1/2}$.

$$\rho_R^{(\mathrm{EG})}(\Gamma^{-1}) \simeq 3\Gamma^2 \mathrm{M_P}^2 \tag{95}$$

which is the standard result. In Fig. 9 we plot the ratio between the reheating temperatures in IG and in EG on varying γ. Such a ratio is obtained on evaluating

$$\frac{T_{\mathrm{reh}}^{(\mathrm{IG})}}{T_{\mathrm{reh}}^{(\mathrm{EG})}} = \left[\frac{\rho_R^{(\mathrm{IG})}(t_{*,\mathrm{IG}})}{\rho_R^{(\mathrm{EG})}(t_{*,\mathrm{EG}})}\right]^{1/4}, \tag{96}$$

where $\rho_R^{(\mathrm{IG})}$ and $\rho_R^{(\mathrm{EG})}$ are the numerical solutions of the exact equations and t_* is the time for which $\rho_R(t_*) = \rho_\sigma(t_*)$, and the comparison is made with the analytical prediction obtained from (94) and (95). Again we observe that the correct behavior is reproduced by our analytical estimates.

VII. PREHEATING

The phenomenological study of reheating described in the previous section was improved by the application of the theory of parametric resonance in an expanding universe to the fields coupled to the inflaton [23,24]. The first stage of the decay of the inflaton—dubbed *preheating*—can be rather efficient and leads to a nonthermal distribution of the decay products. The subsequent nonlinear evolution may end up in thermalizing the content of the Universe.

In this section we study the effect of the parametric resonance for the various types of fluctuations present and coupled to the inflaton during its coherent oscillations. For the analytic treatment we use Eq. (46) for the evolution of the background, and check our results by numerical analysis. For the study of fluctuations during the coherent oscillations regime the cosmic time is useful and one rewrites, through a suitable change of variable, the equations of motion of the diverse fields in a Mathieu-like form:

$$\frac{d^2y(t)}{d(\Omega t)^2} + [A(t) - 2q(t)\sin 2\Omega t]y(t) = 0 \tag{97}$$

where Ω is a frequency which may depend on the field considered. We call the above equation a Mathieu-like equation since in the Mathieu equation A and q do not depend on time. On taking into account the expansion of the Universe A and q depend on time and two principal effects arise: q decays in time and fluctuations, characterized by a comoving momentum k, move in the (q, A) plane (see for example [21]). An examination of the (q, A) plot of the stability/instability regions is useful in order to understand if the (time-)evolution of the modes ends in a stage in which inflaton oscillations cannot be neglected.

The broad resonance regime ($q \gg 1$) has been dubbed *stochastic resonance* in an expanding universe [25]. The intermediate ($q \sim 1$) and narrow ($q \ll 1$) resonance regimes are difficult to treat and the exponential growth which one obtains with A and q constant in time can be completely washed out by the expansion of the Universe. Let us remember that the small q region of the first instability band is

$$1 - q - \frac{q^2}{8} - \mathcal{O}(q^3) < A < 1 + q + \frac{q^2}{8} + \mathcal{O}(q^3), \tag{98}$$

which is situated around $A \simeq 1$. When q is not large the effect of oscillations for y arises mainly if the fluctuation spends time in the first resonant band.

A. Gravitational waves

We begin by considering gravitational waves. The equation governing the dynamics of tensor perturbations (19), on setting $\tilde{h}_k \equiv a^{3/2}\sigma h_k$, can be cast in the form of the Mathieu-like equation

$$\frac{d^2\tilde{h}_k}{dt^2} + m_{\mathrm{eff,t}}(t)^2\tilde{h}_k = 0 \tag{99}$$

and the effective mass is

$$m_{\mathrm{eff,t}}(t)^2 = \omega_0^2\left(\frac{k^2}{a^2\omega_0^2} + \frac{fr}{1 + r\omega_0 t}\sin\omega_0 t\right) + \mathcal{O}\left(\frac{1}{t^2}\right). \tag{100}$$

For $r\omega_0 t \gg 1$ this equation can be rewritten as

$$\frac{d^2\tilde{h}_k}{d(\omega_0 t/2)^2} + [A_h + 2q_h\sin(\omega_0 t)]\tilde{h}_k = 0 \tag{101}$$

where A_h and q_h are time-dependent functions

$$A_h(t) = \frac{4k^2}{a^2\omega_0^2}, \qquad q_h = \frac{f}{2\omega_0 t} \tag{102}$$

and we omit terms of order $1/t^2$. For $r\omega_0 t \gg 1$ the trajectory in the (q, A) plane is therefore $A_h(t) \propto k^2 q_h^{4/3}(t)$. The wavelengths pass through the first resonance band but end in the stability region.

B. Inflaton fluctuations

On considering inflaton mode dynamics for a generic potential (with a nontrivial minimum) Eq. (15) can be recast in the form of a Mathieu-like equation by rescaling $\delta\tilde{\sigma}_k = \sqrt{a^3 Z}\delta\sigma_k$ and keeping contributions of the homogeneous mode fluctuations $\delta\sigma$ to first order. The final equation for $\delta\tilde{\sigma}_k$ turns out to be

$$\frac{d^2\delta\tilde{\sigma}_k}{dt^2} + m_{\mathrm{eff},\sigma}(t)^2\delta\tilde{\sigma}_k = 0 \tag{103}$$

where

$$m_{\mathrm{eff,s}}(t)^2 \equiv \omega_0^2\left[1 - \frac{9fr}{1 + r\omega_0 t}\cos\omega_0 t \times \left(1 + \frac{4\sqrt{6\gamma(1+6\gamma)}}{9\gamma}\sin\omega_0 t\right)\right] + \mathcal{O}\left(\frac{1}{t^2}\right) \tag{104}$$

and f and r are defined in (59). Thus, in the $r\omega_0 t \gg 1$

regime, Eq. (103) reduces to

$$\frac{d^2\delta\tilde{\sigma}_k}{d(\omega_0 t)^2} + [A_\sigma + 2q_{\sigma 1}\sin(2\omega_0 t) + 2q_{\sigma 2}\sin(\omega_0 t)]\delta\tilde{\sigma}_k = 0 \tag{105}$$

where A_σ, $q_{\sigma 1}$ and $q_{\sigma 2}$ are time-dependent functions of the form

$$A_\sigma = \frac{k^2}{a^2\omega_0^2} + 1, \qquad q_{\sigma 1} = \frac{2}{\omega_0 t}, \qquad q_{\sigma 2} = \frac{\sqrt{\frac{27\gamma}{2(1+6\gamma)}}}{\omega_0 t} \tag{106}$$

and we omit terms of order $1/t^2$. The equation for the rescaled IG inflaton fluctuations therefore exhibits two oscillating terms: whereas the one multiplied by $q_{\sigma 2}$ is similar to the term appearing for gravitational waves, $q_{\sigma 1}$ does not depend on γ. On neglecting $q_{\sigma 2}$ one has the following trajectory in the (q, A) plane:

$$A_\sigma(t) = 1 + \frac{k^2}{a^2\omega_0^2} = 1 + \frac{k^2}{a_0^2\omega_0^2}\left(\frac{\omega_0 t_0}{2}\right)^{4/3} q_{\sigma 1}^{4/3}(t), \tag{107}$$

which shows how fluctuations end in the first resonance band asymptotically. The fluctuation $\delta\tilde{\sigma}_k$ grows linearly in time as shown carefully by the MSA method in the Appendix. This means that the inflaton fluctuations oscillate with constant amplitude [9], rather than decay if oscillations in the homogeneous inflaton are averaged in time. Since $q_{\sigma 1}$ does not depend on γ our analysis applies to the coherent oscillation regime of chaotic quadratic inflation in Einstein gravity as well, in agreement with Ref. [26]. Therefore during the coherent oscillations of a massive inflaton, gauge-invariant inflaton fluctuations oscillate with constant amplitude on large scales [27] and also on small scales. We have numerically checked that the inclusion of the oscillation term multiplied by $q_{\sigma 2}$ does not modify the qualitative behavior just described. Indeed the amplitude of this term is never important, $q_{\sigma 2} \sim \mathcal{O}(\gamma/(\omega_0 t))$ for $\gamma \ll 1$ and $q_{\sigma 2} \sim 3/(2\omega_0 t)$ for $\gamma \gg 1$, and the frequency of oscillations is half of the dominant one.

C. Scalar fields nonminimally coupled to gravity

We finally take into consideration the evolution of a scalar test field χ nonminimally coupled to gravity and interacting with the inflaton. Let

$$S_\chi = \int dx^4\sqrt{-g}\left[-\frac{g^{\mu\nu}}{2}\partial_\mu\chi\partial_\nu\chi - \frac{m_\chi^2}{2}\chi^2 + \mathcal{L}_{\rm int}\right] \tag{108}$$

be the action for such a field and

$$\mathcal{L}_{\rm int} = -\frac{\xi}{2}R\chi^2 + \frac{g^2}{2}\sigma^2\chi^2 \tag{109}$$

the interaction with $\xi > 0$. On considering only the interaction of the modes of the field χ with the homogeneous part of the inflaton one finally obtains

$$\frac{d^2\tilde{\chi}_k}{dt^2} + m_{{\rm eff},\chi}(t)^2\tilde{\chi}_k = 0 \tag{110}$$

where

$$m_{{\rm eff},\chi}(t)^2 = \omega_0^2\left[\frac{k^2}{a^2\omega_0^2} + \frac{3(4\xi-1)fr}{1+r\omega_0 t}\sin\omega_0 t + 2g^2\frac{1+6\gamma}{\mu}\frac{fr}{1+r\omega_0 t}\sin\omega_0 t + \frac{m_\chi^2}{\omega_0^2} + g^2\frac{1+6\gamma}{2\mu}\right] + \mathcal{O}\left(\frac{1}{t^2}\right) \tag{111}$$

and $\tilde{\chi}_k = a^{3/2}\chi_k$. From (111) we see that the scalar field does not end up in the instability region unless

$$\frac{m_\chi^2}{\omega_0^2} + g^2\frac{1+6\gamma}{2\mu} \simeq \frac{1}{2}, \tag{112}$$

which shows how a mass m_χ^2 generically suppresses the resonance. Note also that a broad resonance regime is possible for $m_\chi = g = 0$ for large ξ.

VIII. CONCLUSIONS

We have investigated in detail inflation in the IG framework where inflation is driven by the same scalar field as that associated with the observed value of Newton's constant. Inflation in IG can be successful in the SR regime, and leads to a nearly flat spectrum of scalar perturbations and a small tensor-to-scalar ratio compatibly with observations. The SR conditions are not simply associated with the shape of the inflaton potential since the dynamics of the scalar field strongly depends on its coupling γ to gravity. We have made accurate comparisons with observations for different "symmetry-breaking" potentials and showed how their shape is relevant for successful predictions of the model. In particular we have seen that the LG and CW type potentials are compatible with the data for large field inflation and for suitable values of the parameters for small field inflation. For potentials involving higher powers of the scalar field (with respect to the previously mentioned cases) agreement with the data is more problematic and if it occurs one obtains constraints on γ for both the large and small field cases.

We have also studied, always in IG, the coherent oscillatory regime and obtained an accurate analytical solution for the dynamics of the inflaton and of the Hubble parameter by using an MSA. We employed the solution to first investigate the behavior of the average evolution of the Universe. We found that, independently of the average equation of state of the scalar field, the Universe expands as $\langle H(t)\rangle \propto 2/(3t)$.

Further perturbative and resonant reheating have also been studied. We found, in the former case, that the decay

of the inflaton into ordinary matter is less efficient for γ large and that the reheating temperature is comparable with the EG value for γ small. We also examined the parametric amplification of the scalar and tensor perturbations and of a generic scalar field nonminimally coupled to gravity and coupled to the inflaton. We note that parametric resonance occurs for scalar perturbations with $H \ll k/a \ll \omega_0$ and such perturbations maintain a constant amplitude instead of decaying as the Universe expands. Finally parametric resonance does not occur for gravitational waves whereas amplification may occur for a generic scalar field depending on the parameters of its Lagrangian.

APPENDIX A: PREHEATING

In an expanding space-time, parametric resonance in the first instability band occurs when the Mathieu-like equation governing modes dynamics can be cast in the form

$$\ddot{y} + [1 + \epsilon q(t)\sin 2t]y = 0 \tag{A1}$$

where ϵ is a small dimensionless parameter. The theory of parametric resonance is well known when $q(t) = \text{const}$ but in an expanding space-time, where a time dependence generally appears, the dynamics leads to quite different results. MSA gives the correct approximate behavior for (A1).

Since $\epsilon q(t) \ll 1$ one can look for an approximate solution in the form

$$y = y_0(t, \tau) + \epsilon y_1(t, \tau) \tag{A2}$$

where $\tau \equiv \epsilon t$. On comparing orders one has

$$\frac{\partial^2 y_0}{\partial t^2} + y_0 = 0 \Rightarrow y_0 = A(\tau)e^{it} + \text{c.c.} \tag{A3}$$

$$\frac{\partial^2 y_1}{\partial t^2} + y_1 + 2\frac{\partial^2 y_0}{\partial t \partial \tau} + q(t)\frac{e^{2it} - e^{-2it}}{2i}y_0 = 0 \tag{A4}$$

and the requirement that secular contributions cancel in (A4) leads to the differential equation

$$4\frac{dA}{dt} - q(t)A^* = 0. \tag{A5}$$

On separating A into real and imaginary parts ($A = B + iC$) growing and decaying modes also separate

$$4\frac{dB}{dt} - q(t)B = 0 \tag{A6}$$

$$4\frac{dC}{dt} + q(t)C = 0 \tag{A7}$$

and, if $q(t) > 0$, the imaginary part decays.

In general, the expansion of the Universe during reheating leads to $q(t) \sim p/t^n$ and in this case the growing dynamics becomes

$$B(t) = B_0 \exp \int_{t_0}^{t} \frac{p}{4\tilde{t}^n} d\tilde{t}. \tag{A8}$$

When $n > 1$ the amplitude of oscillations increases but still exhibits a constant asymptotic behavior $B \sim B_0 \exp[\frac{p}{4(n-1)} t_0^{1-n}]$, for $n < 1$ the amplitude increases exponentially as $B \sim B_0 \exp[\frac{p}{4(1-n)} t^{1-n}]$. In contrast, when $n = 1$ (which is the value we find for scalar perturbations in the instability region), one obtains the following power-law dependence:

$$B = B_0\left(\frac{t}{t_0}\right)^{p/4} \tag{A9}$$

which, for $p = 4$ corresponds to $\delta\tilde{\sigma} \sim t$, as mentioned in Sec. VII B.

[1] C. Brans and R. H. Dicke, Phys. Rev. **124**, 925 (1961).
[2] A. D. Sakharov, Dokl. Akad. Nauk SSSR **177**, 70 (1967) [Sov. Phys. Dokl. **12**, 1040 (1968)].
[3] A. Zee, Phys. Rev. D **23**, 858 (1981).
[4] S. Adler, Rev. Mod. Phys. **54**, 729 (1982).
[5] F. Cooper and G. Venturi, Phys. Rev. D **24**, 3338 (1981).
[6] A. Zee, Phys. Rev. Lett. **42**, 417 (1979).
[7] F. S. Accetta, D. J. Zoller, and M. S. Turner, Phys. Rev. D **31**, 3046 (1985).
[8] N. Kaloper, L. Sorbo, and J. Yokoyama, Phys. Rev. D **78**, 043527 (2008).
[9] S. R. Coleman and E. J. Weinberg, Phys. Rev. D **7**, 1888 (1973).
[10] B. L. Spokoiny, Phys. Lett. B **147**, 39 (1984).
[11] F. Finelli, A. Tronconi, and G. Venturi, Phys. Lett. B **659**, 466 (2008).
[12] A. Cerioni, F. Finelli, A. Tronconi, and G. Venturi, Phys. Lett. B **681**, 383 (2009).
[13] K. i. Maeda, Phys. Rev. D **39**, 3159 (1989).
[14] E. E. Flanagan, Classical Quantum Gravity **21**, 3817 (2004).
[15] T. Chiba and M. Yamaguchi, J. Cosmol. Astropart. Phys. 10 (2008) 021.
[16] J. c. Hwang, Classical Quantum Gravity **14**, 3327 (1997).
[17] F. Finelli, J. Hamann, S. M. Leach, and J. Lesgourgues, J. Cosmol. Astropart. Phys. 04 (2010) 011.
[18] E. Komatsu *et al.* (WMAP Collaboration), Astrophys. J. Suppl. Ser. **180**, 330 (2009).

[19] This result differs from that presented previously [12]. The reason is that the initial position of the field for SF inflation depends on the choice of γ. Indeed for sufficiently small γ a small shift of the inflaton from the minimum is sufficient to guarantee the necessary inflation, therefore we have expanded about the minimum.
[20] M. S. Turner, Phys. Rev. D **28**, 1243 (1983).
[21] C. M. Bender and S. A. Orszag, *Advanced Mathematical Methods for Scientists and Engineers: Asymptotic Methods and Perturbation Theory* (Springer Verlag, New York, 1999).
[22] ρ_R is negligible at the beginning of the reheating era and increases becoming comparable with ρ_σ.
[23] J. H. Traschen and R. H. Brandenberger, Phys. Rev. D **42**, 2491 (1990).
[24] L. Kofman, A. D. Linde, and A. A. Starobinsky, Phys. Rev. Lett. **73**, 3195 (1994).
[25] L. Kofman, A. D. Linde, and A. A. Starobinsky, Phys. Rev. D **56**, 3258 (1997).
[26] Y. Nambu and A. Taruya, Prog. Theor. Phys. **97**, 83 (1997).
[27] F. Finelli and R. H. Brandenberger, Phys. Rev. Lett. **82**, 1362 (1999).